DOI: 10.1002/chem.200701302

Synthesis, Self-Assembling Properties, and Atom Transfer Radical Polymerization of Alkylated L-Phenylalanine-Derived Monomeric Organogel from Silica: A New Approach To Prepare Packing Materials for High-Performance Liquid Chromatography

M. Mizanur Rahman, Miklós Czaun, Makoto Takafuji, and Hirotaka Ihara*[a]

Abstract: The monomer *N'*-octadecyl-N^{α}-(4-vinyl)-benzoyl-L-phenylalanineamide (**4**) based on L-phenylalanine has been simply but effectively synthesized, and its self-assembling properties have been investigated. FTIR and a variable-temperature ^{1}H NMR spectroscopic investigation demonstrated that the aggregation of compound **4** in various organic solvents is due to the formation of intermolecular hydrogen bonds among the amide moieties. UV/Vis measurements indicated that the multiple π–π interactions of the phenyl groups also contribute to the self-assembly. As was observed by ^{13}C cross-polarization magic-angle spinning (CP/MAS) NMR and variable-temperature ^{1}H NMR measurements, the ordered alkyl chains also played an important role in the molecular aggregation by van der Waals interactions. Compound **4** was polymerized by surface-initiated atom transfer radical polymerization from porous silica gel to prepare a packing material for HPLC. The results of thermogravimetric analysis showed that a relatively large amount of polymer was grafted onto the silica surface. The organic phase on silica was in a noncrystalline solid form in which the long alkyl chain exists in a less-ordered *gauche* conformation. Analysis of chromatographic performance for polyaromatic hydrocarbon samples showed higher selectivity than conventional reversed-phase HPLC packing materials.

Keywords: gels · liquid chromatography · polyaromatic hydrocarbons · polymerization · self-assembly

Introduction

In recent years, there has been renewed interest in synthetic polypeptides because of their potential application as biodegradable and biomedical polymers,[1] as well as their ability to form highly ordered hierarchical structures through noncovalent forces such as hydrogen bonding.[2] Incorporation of a high degree of amino acid functionality and chirality in polymer chains can enhance the potential to form secondary structures (α helix and β sheet) and higher-ordered structures.[3] These synthetic polymers can be useful as chiral recognition stationary phases for HPLC,[4] metal-ion absorbents,[5] drug-delivery agents,[6] and biocompatible materials.[7] Such characteristic self-assembled structures and the potential applications of polymers derived from amino acids have attracted researchers to develop new synthetic routes to prepare a wide variety of amino acid based polymers by using various polymerization techniques.[8]

In principle, the formation of polymer-grafted inorganic particles can be approached in two ways. 1) The "grafting to" technique[9] consists of the synthesis of end-functionalized polymers followed by the immobilization of these polymers onto the surface through anchoring groups. The "grafting to" method is experimentally simple but it has a limitation, namely the difficulty in achieving high grafting density because of the steric crowding of the surface by the already grafted polymers.[10] 2) On the contrary, in surface-initiated polymerization ("grafting from") polymer chains grow in situ from initiator molecules that have been pregrafted to the surface of inorganic particles.[11] The "grafting from" approach is considered to give higher densities because only monomer molecules have to diffuse to the active species.

"Living"/controlled radical polymerization (CRP) methods, such as nitroxide-mediated polymerization (NMP), atom transfer radical polymerization (ATRP), reversible ad-

[a] Dr. M. M. Rahman, Dr. M. Czaun, Dr. M. Takafuji, Prof. H. Ihara
Applied Chemistry and Biochemistry
Kumamoto University
2-39-1 Kurokami, Kumamoto 860-8555 (Japan)
Fax: (+81) 96-342-3662
E-mail: ihara@kumamoto-u.ac.jp

Supporting information for this article is available on the WWW under http://www.chemeurj.org/ or from the author.

dition–fragmentation chain transfer (RAFT) polymerization, living anionic polymerization (LAP), and living cationic polymerization (LCP), provide an ability to produce particular polymer architectures with controlled molecular weight and molecular weight distributions.[12] The major difference between the conventional radical polymerization techniques and CRP is the lifetime of the propagating radicals. While radicals derived from the thermal decomposition of conventional radical polymerization initiators (azobisisobutyronitrile type) may undergo termination reactions within a few seconds, the lifetime of the propagating radicals can be extended to several hours in controlled processes.[13] Among the CRP processes, increasing attention has been paid to ATRP since its discovery by Matyjaszewski and Sawamoto,[14] because this method does not require rigorous experimental conditions like LAP or LCP.

The reaction between the activator complex (often CuBr-chelated by N-donor ligands) and the dormant initiator results in the formation of a propagating radical and deactivator complex by a reversible halogen-atom transfer reaction (Scheme 1). A low stationary concentration of propagating

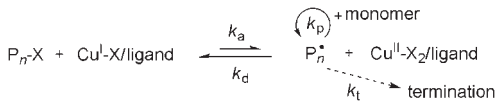

Scheme 1. Mechanism of ATRP.

radical ($<10^{-8}$ M) is maintained by the dynamic equilibrium which is established after a short period of time (in a few seconds).[13] Recent advances in controlled/living polymerization processes have encouraged the preparation of a multitude of macromolecules with controllable architecture, functionality, composition, and topology.[15]

The use of amino acid based assemblies as delivery vehicles is induced principally by their ability to incorporate and release poorly water-soluble, hydrophobic, and/or highly toxic compounds, while also minimizing drug degradation and wastage, and hence increasing bioavailability.[16] To date there is no report on the synthesis, self-assembling properties, and surface-initiated ATRP of alkyl L-phenylalanine-derived monomers. Herein, we present the synthesis, characterization, and subsequent polymerization of an alkyl L-phenylalanine monomer from ATRP initiator-grafted silica particles. Furthermore, an application of these polymer-coated silica particles as a stationary phase for HPLC is introduced.

Results and Discussion

Synthesis of *N′*-octadecyl-*N*$^{\alpha}$-(4-vinyl)-benzoyl-L-phenylalanineamide: We selected L-phenylalanine as chiral origin due to its neutral character to avoid synthetic difficulty and because of its high hydrophobicity. Scheme 2 illustrates the synthetic process of the L-phenylalanine derivatives. *N*-Benzyloxycarbonyl-L-phenylalanine (**1**), derived from L-phenylalanine and Z-Cl, was reacted with stearylamine in THF in the presence of a peptide synthesis coupling agent DEPC, affording *N′*-octadecyl-*N*$^{\alpha}$-carbobenzoyl-L-phenylalanineamide (**2**). Deprotection of the α-amino group of **2** by hydrogenation (catalyzed by Pd/carbon black) resulted in *N′*-octadecyl-L-phenylalanineamide (**3**). The acylation of the α-amino group was carried out with 4-vinylbenzoic acid in alkaline medium in the presence of DEPC in THF at 0 °C, to give the octadecylated L-phenylalanine-derived monomer **4** as a white powder. The characterization of **1**–**4** was carried out by elemental analysis and different spectroscopic methods (see Figures S1 and S2 in the Supporting Information). Compound **4** was then used for surface-initiated living radical polymerization from a silica surface to produce a high-density chromatographic stationary phase.

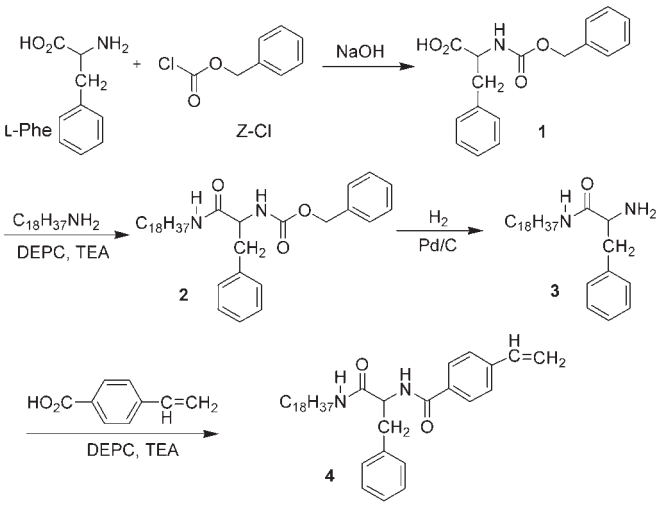

Scheme 2. Synthesis of compound **4** from L-phenylalanine (L-Phe). Z-Cl: carbobenzoxy chloride; DEPC: diethylphosphorocyanidate; TEA: triethylamine.

Self-assembling properties of compound 4: It is well known that hydrogen bonding is one of the driving forces for self-assembly of organogelators in organic solvents.[17] IR and ^{1}H NMR spectroscopies are powerful tools to study hydrogen-bonding interactions. Extensive precedent indicates that secondary amide groups (NH) engaged in the standard amide–amide hydrogen bonds (C=O···H–N) display stretching bands in the range 3370–3250 cm^{-1}, while stretching bands in the range 3500–3400 cm^{-1} are attributed to "free" secondary amide groups that are not involved in hydrogen bonding.[18] The FTIR spectrum of compound **4** in $CHCl_3$, in which no self-assembly occurs, showed an absorption band at 3434 cm^{-1} attributed to free N–H groups[19] (Figure S3, Supporting Information). On the other hand, the FTIR spectrum of **4** in a cyclohexane gel ([**4**] = 30 mM) showed absorption bands at 3302 cm^{-1} as well as 1658 and 1631 cm^{-1}, arising from the intermolecular hydrogen-bonded amide moieties (Figure S4, Supporting Information). The FTIR measurements also provide information on the alkyl groups. The absorption bands of the antisymmetric (ν_{as}) and sym-

metric (ν_s) CH_2 stretching vibrations of **4** appeared at 2927 (ν_{as}, CH_2) and 2855 cm^{-1} (ν_s, CH_2) in $CHCl_3$, while in the benzene gel they shifted to 2919 and 2850 cm^{-1}, respectively (Figure S5, Supporting Information). Such a frequency shift to lower wavenumbers is induced by the restricted mobility of the alkyl chains in **4**, thus indicating that van der Waals interactions among the alkyl chains also plays an important role in the self-assembly of **4** molecules.[20]

Figure 1 shows variable-temperature ^1H NMR measurements of compound **4** in [D_{12}]cyclohexane gel from 30 to

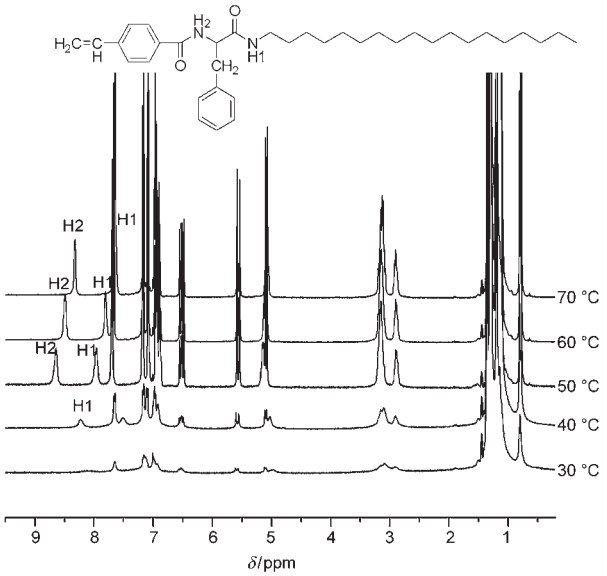

Figure 1. Partial ^1H NMR spectra of compound **4** in [D_{12}]cyclohexane gel, indicating the shift of amide protons.

70 °C with the assignments of key amide protons: *N*-alkylamide (H1) and the α-amide (H2). As the temperature increased, the peaks for amide protons were consistently visible as representative of the associated amide function. Upon increasing the temperature, the intensity of the two bands increased and shifted upfield, demonstrating the presence of one-mode association alternation between the free and the associated species. The intensity of the peaks ascribed to the aliphatic moieties at $\delta = 1.2$ ppm also increased within the temperature range of 30 to 70 °C and became sharper gradually, which suggests that the mobility of the alkyl chain increases as a function of temperature (Figure S6, Supporting Information). The ordered structural conformation of the alkyl chain of **4** was evaluated by ^{13}C cross-polarization magic-angle spinning (CP/MAS) NMR measurements (Figure 2). The higher intensity of the peak at $\delta = 33.4$ ppm attributed to the *trans* conformation indicates that most of the alkyl chains are in an ordered structure at ambient temperature.[21]

To monitor the interaction between the phenyl groups of **4**, UV/Vis spectra were collected in cyclohexane at variable temperature (80–0 °C). The intensity of the absorption band at 262 nm decreased as the temperature fell, providing clear

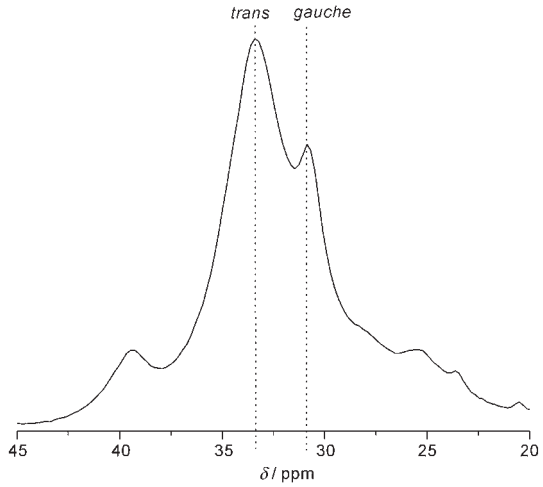

Figure 2. Partial ^{13}C CP/MAS NMR spectrum of compound **4** at room temperature.

evidence that the aromatic moieties also aggregate through π–π interactions (Figure S7, Supporting Information). The FTIR, NMR, and UV/Vis measurements demonstrated that intermolecular hydrogen bonding among the amide moieties, van der Waals interaction between the alkyl chains, and π–π interactions of the aromatic groups played the most important roles in the self-assembly of compound **4**. The molecular packing model of compound **4** was estimated by HyperChem version 5.1 with molecular mechanics by using the semiempirical AM1 method (Figure 3). Calculations were

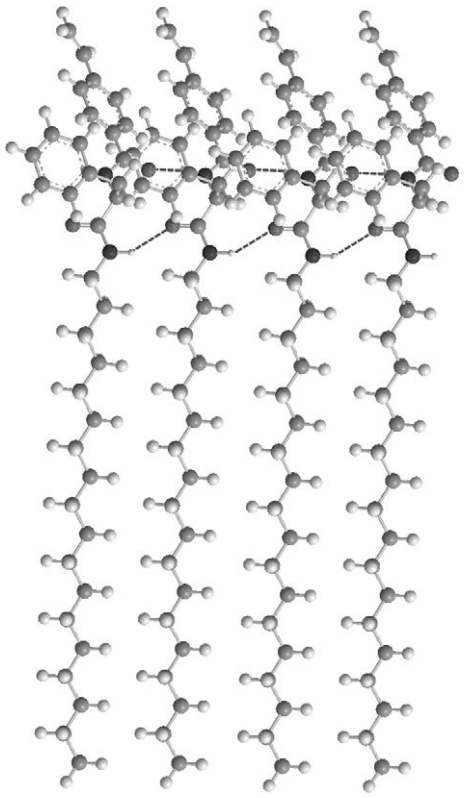

Figure 3. Molecular packing model of compound **4**.

stopped when the difference in the energy level after two consecutive iterations was less than 0.001 kcal mol^{-1}. The computer simulation confirmed the experimental results, namely the driving force for the self-assembly of **4** is partly based on the intermolecular hydrogen bonding between the oxygen atom derived from the carbonyl group and the nitrogen atom of the amide moiety. Indeed, it can be described by the two symmetrical hydrogen bonds between the amide nitrogen and carbonyl oxygen atoms of the L-phenylalanine moiety, and furthermore between the α-amide nitrogen and the carbonyl oxygen atoms of the 4-vinylbenzoyl moiety.

Chromatographic application of molecular gels: We have reported the development of a poly(octadecyl acrylate) derivative as a lipid membrane analogue and its successful application as a HPLC stationary phase after immobilization onto silica. Our detailed investigations revealed that the highly ordered structure induced the orientation of the carbonyl groups that work as a source of π–π interaction between the stationary phase and the solute molecules. The aligned carbonyl groups provide effective recognition of the molecular planarity and linearity of polyaromatic hydrocarbons (PAHs) through multiple π–π interactions.[22] We have also reported that dialkyl L-glutamide-derived amphiphilic lipids form nanotubes, nanohelices, and nanofibers induced by the bilayer structures in water or organic solvents, and by intermolecular hydrogen bonds among the amide moieties that also contribute to self-assembly.[23] Successful application of a dialkyl L-glutamide-derived organogel as a HPLC stationary phase revealed that the highly ordered molecules form a condensed thin layer over the silica surface by intermolecular hydrogen bonding among the amide moieties, which keeps the carbonyl groups in an ordered form favorable for multiple π–π interactions with the guest molecule. Enhanced molecular shape selectivity was observed through π–π interactions between the carbonyl groups and the delocalized electrons of PAHs for the glutamide-derived stationary phase.[24] As similar noncovalent interactions, namely hydrogen bonding among the amide moieties and aromatic π–π interactions, were found to contribute to the self-assembly of compound **4**, Sil-poly**4** (Scheme 3) could be considered as a novel stationary phase for HPLC applications.

Polymerization of 4 from silica by surface-initiated ATRP: To synthesize polymer-grafted silica particles we broke the process down into two steps (Scheme 3): 1) immobilization of ATRP initiator on silica particles and 2) polymerization from initiator-grafted silica. Radical polymerization initiator [11-(2-bromo-2-methyl)propionyloxy]undecyltrichlorosilane (**5**) was synthesized according to a method reported in the literature.[25] Initiator **5** was grafted onto silica in dry toluene in the presence of TEA under a nitrogen atmosphere (see Experimental Section). The reaction between the surface-accessible OH group of silica and the anchoring group of the initiator (−$SiCl_3$) resulted in the formation of a chemical bond between the silica surface and initiator **5** (Sil-**5**). ATRP processes were carried out by using Sil-**5** as a macroinitiator suspended in the mixture of monomer and toluene in the presence of CuBr and PMDETA as catalyst precursors (see the Supporting Information). After the ATRP process, Sil-poly**4** was purified by repeated washing in different solvents to remove the nongrafted polymers from the surface. Structural characterization of Sil-**5** and Sil-poly**4** was carried out by different spectroscopic (diffuse reflectance infrared Fourier transform (DRIFT), NMR) and thermoanalytic methods (thermogravimetric analysis (TGA)).

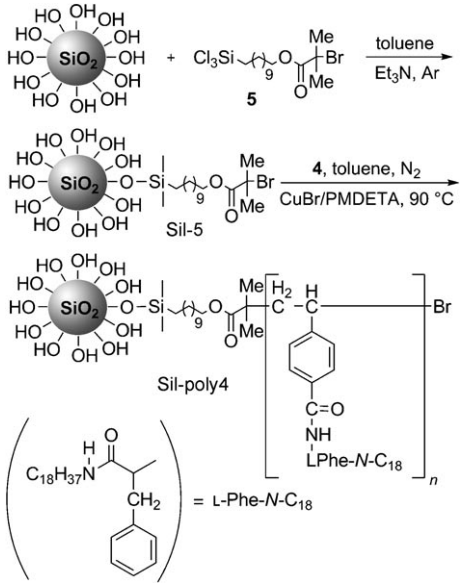

Scheme 3. Synthetic steps for the preparation of poly**4**-grafted silica particles (Sil-poly**4**). PMDETA: 1,1,4,7,7-pentamethyldiethylenetriamine.

Thermogravimetric analysis of Sil-poly4: To assess the organic content of the initiator-functionalized and polymer-modified silica, repeated TGA runs were conducted and almost identical curves were obtained. As the good reproducibility does not prove that significant errors are not incurred, control TGA experiments with nongrafted poly**4** were needed. Before measurements, each sample was first kept under vacuum at 35 °C for 5 h to remove solvent traces, then TGA measurements were run at a constant heating rate of 10 °C min^{-1} in air by using an empty crucible as a reference. The heating process was carried out up to 800 °C, which has been demonstrated to be sufficiently high to degrade all surface-bonded organosilanes.[26] Typical TGA curves for the bare silica, Sil-**5**, and Sil-poly**4** are depicted in Figure 4.

The weight retention profile of Sil-**5** reached a plateau at 110 °C (drying period), indicating the removal of surface water. After the thermal degradation of the initiator the weight of the sample was constant from 650 to 800 °C.

A plateau in the weight retention curve of Sil-poly**4** was also observed as the temperature reached 600 °C, confirming that there is no polymer material remaining on the silica at 800 °C. Considering the TGA curve of Sil-**5** as reference, the weight of the immobilized initiator can be calculated as 9.6 wt % of the total mass. Similarly, TGA revealed that

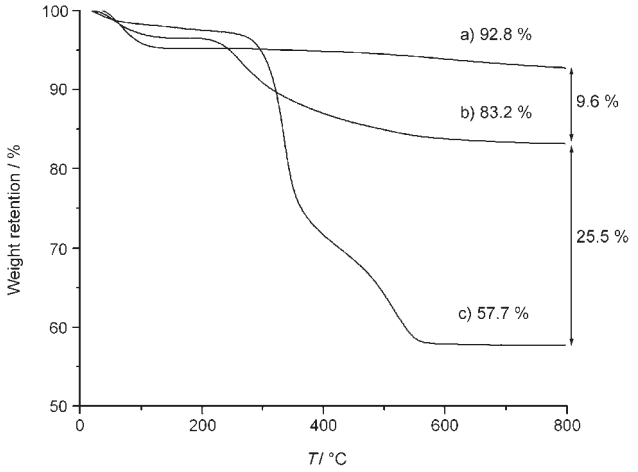

Figure 4. TGA curves for a) bare silica particles, b) Sil-**5**, and c) Sil-poly**4**.

25.5 wt% poly**4** is grafted on the silica surface if the weight retention of Sil-**5** was considered as reference at 800 °C. The former weight difference (9.6%) was translated into an average grafting density of 0.61 initiator molecules per nm^2. However, this value is one order of magnitude lower than the generally accepted silica surface hydroxyl group density (five OH groups per nm^2)[27] but slightly higher than that demonstrated in other reports.[28] From the results of TGA measurements it can be concluded that a fairly large amount of polymer was grafted onto the silica surface by the ATRP process, and Sil-poly**4** can be considered as a high-density organic phase for HPLC.

IR analysis: Immobilization of ATRP initiator **5** and surface-initiated polymerization of **4** were also confirmed by DRIFT spectroscopy. The absorbance spectra for bare silica particles, Sil-**5**, and Sil-poly**4** in the region from 3700 to 1500 cm^{-1} are shown in Figure 5. In spectrum b, the ester group introduced by initiator **5** is clearly noticeable, as indicated by the C=O bond stretching at 1717 cm^{-1}. A group of peaks at 2931 and 2859 cm^{-1} is attributed to the CH bond stretching of the long alkyl chain in initiator **5**. The FTIR spectrum of **4** (Figure 5, spectrum d) shows intense bands at 1659 and 1630 cm^{-1} corresponding to the carbonyl stretching of the two amide bonds, respectively (the latter overlapped with the C=C stretching band of the vinyl moiety). A broad signal (Figure 5, spectrum c) could be observed at 1634 cm^{-1}, indicating the presence of grafted polymer. The spectrum of Sil-poly**4** also displays a peak at 1719 cm^{-1} due to the carbonyl stretching of initiator **5**, but the intensity in this case is not as strong as that detected in the spectrum of Sil-**5**. Equally important is the appearance of N–H stretching (3293 cm^{-1}) in spectrum c derived from poly**4**, providing further evidence that monomer **4** was successfully polymerized from the silica surface. The Si–OH bonds of the pure silica show an absorption band at 3652 cm^{-1}, indicating that some surface OH groups remained unfunctionalized (Figure 5a and c). These results clearly proved that a considerably large amount of poly**4** could be immobilized on the silica surface.

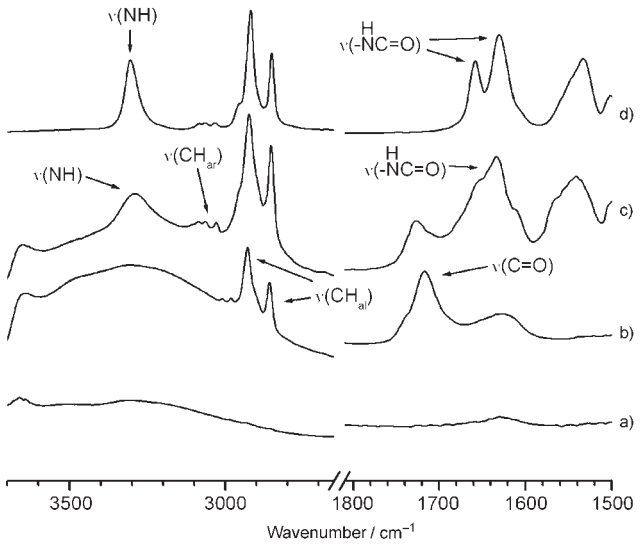

Figure 5. DRIFT spectra of a) bare silica particles, b) Sil-**5**, and c) Sil-poly**4**; d) FTIR spectrum of **4**.

NMR studies of Sil-poly4: In liquid- or suspended-state NMR spectroscopy, only those molecules or parts of molecules are detectable that have very fast rotational motions.[29] The motion must be in such a fast range that it can average out dipolar coupling and chemical shift anisotropy until the related NMR peaks become narrow enough to be detected. The suspension-state ^1H NMR spectroscopy of Sil-poly**4** was measured from 25 to 50 °C. Neither the half-height width (line width) of methylene groups nor the spin–spin relaxation time (T^2) showed any significant change with temperature (20–50 °C). We observed that the intensity of the NMR peaks representing terminal methyl and methylene groups of octadecyl moieties increased slightly and were detectable when a very high vertical scale was used for graphical presentation. These results indicate that the organic phase on the silica surface is in the solid state at room temperature.

Solid-state ^{13}C CP/MAS NMR spectroscopy is a powerful tool for evaluation of the chemical composition of modified surfaces and for confirming the integrity of the immobilized alkyl groups. ^{13}C CP/MAS NMR spectra of Sil-poly**4** were acquired at variable temperature (25–50 °C). It is well known that the ^{13}C NMR signals for $(CH_2)_n$ carbon atoms appear at two resonances, one at $\delta = 32.2$ ppm due to the *trans* conformation, indicating the presence of rigid and ordered chains, and the other at $\delta = 30.0$ ppm due to the *gauche* conformation.[21] The intense signal at $\delta = 29.9$ ppm in the ^{13}C CP/MAS NMR spectra, attributed to the methylene carbon atoms of the octadecyl groups, indicates that the *N*-alkyl chains of Sil-poly**4** are arranged in a less ordered *gauche* conformational form, and no alteration to the ordered *trans* conformation could be observed in the temperature range 25–50 °C (Figure S8, Supporting Information).

^{29}Si CP/MAS NMR investigation shows the differentiation between geminal silanol groups (Q^2) and free silanol groups (Q^3) besides the siloxane groups (Q^4), which are indicated by signals at $\delta = -92$, -102, and -111 ppm, respectively. In initiator- and polymer-grafted silica the signal corresponding to residual geminal silanols is not seen. When the initiator was reacted with the silica surface, a large amount of cross-linked T^2-type silicon species ($\delta = -57$ ppm) was observed while polymer grafting increased the cross-linked surface, as indicated by the appearance of T^3 signals ($\delta = -65$ ppm) and the absence of a signal for T^1[30] (^{29}Si CP/MAS NMR spectra are given in Figure S9 in the Supporting Information).

To demonstrate an application of the new amino acid derived monomer, Sil-poly**4** was suspended in chloroform/hexanol and packed in a stainless-steel column of length 25 cm and internal diameter (i.d.) 4.6 mm by using methanol as packing solvent. The packed column was used for chromatographic analysis and the results are described in the following sections.

Retention mode: It is known that conventional octadecylsilane (ODS) or alkyl phases can recognize the hydrophobicity of analytes in HPLC, and this hydrophobicity is measured by the methylene activity of the stationary phases. This activity reflects the possibility of the phase being able to separate two molecules that differ only in methylene groups, for example, amylbenzene and butylbenzene or ethylbenzene and toluene. The retention mode, as well as the extent of hydrophobic interaction among the analytes and the packing materials in HPLC, can be determined by retention studies of alkylbenzenes.[31]

To evaluate the retention mode and chromatographic performance, Sil-poly**4** was packed in a stainless-steel column and separation experiments were carried out. Figure 6 shows the correlation between $\log k$ and $\log P$ for Sil-poly**4** and a conventional ODS phase. Notably, the retention mode of Sil-poly**4** showed a reversed-phase mode compared to that of the conventional ODS phase. As indicated in Figure 6, this phase showed a much higher retention for both alkylbenzenes and PAHs. It was also observed that $\log k$ and $\log P$ plots of alkylbenzenes and PAHs in ODS were parallel and almost coincided with each other, providing evidence that ODS can recognize only the hydrophobicity of analytes.

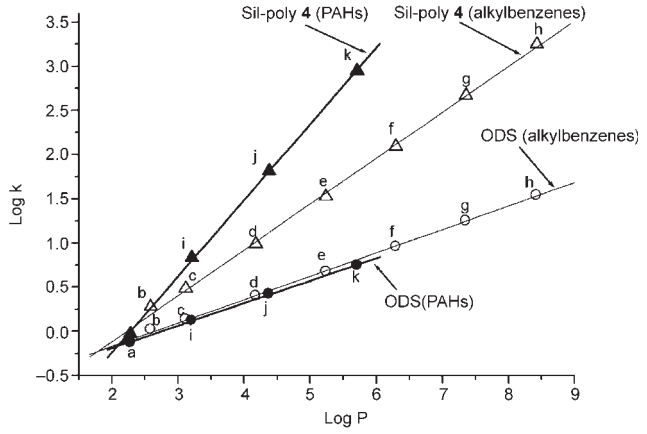

Figure 6. Log k versus log P plots for ODS and Sil-poly**4** stationary phases; a: benzene, b: toluene, c: ethylbenzene, d: butylbenzene, e: hexylbenzene, f: octylbenzene, g: decylbenzene, h: dodecylbenzene, i: naphthalene, j: anthracene, k: naphthacene.

It was found that Sil-poly**4** showed a higher retention for PAHs compared to its values for alkylbenzenes. For instance, the $\log P$ of naphthacene (5.71) is smaller than that of octylbenzene (6.30), while the $\log k$ value of naphthacene (2.95) is higher than that of octylbenzene (2.09). The increase of $\log k$ for PAHs was accompanied by selectivity enhancement, which provides specific interactive sites for PAHs that can recognize aromaticity as well as molecular hydrophobicity.

Chromatographic performance of Sil-poly4: The first chromatographic evaluation was performed by using the Tanaka test mixture containing hydrophobic probes.[32] Figure 7 shows the chromatogram obtained, in which it can be observed that all compounds were separated with good efficiencies and good peak shapes. This characterization protocol is a well-developed approach that is recommended to obtain information about the functionality of the silyl reagent and the methylene selectivity, as well as to establish the repeatability and reproducibility of the separation behavior of commercially available reversed phases.[32] The most relevant properties, which are measured by the chromatographic parameters for the separation of seven compounds, are shape and methylene selectivities, hydrogen bonding, and ion-exchange capacities in neutral media.

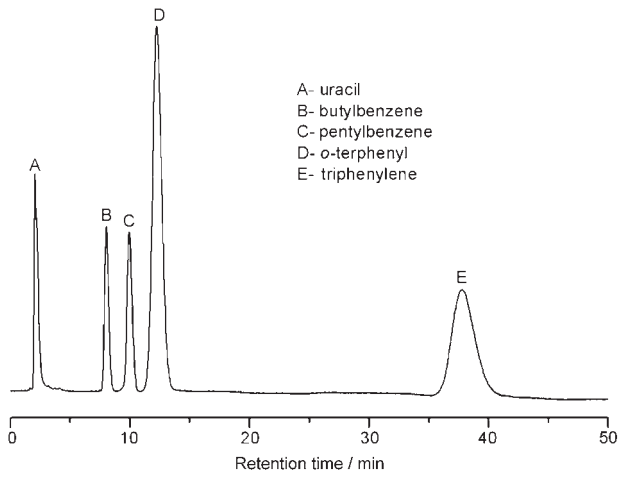

Figure 7. Chromatogram for Tanaka test mixture with Sil-poly**4**. Mobile phase: MeOH/H_2O (90:10), flow rate: 1 mL min^{-1}, column temperature: 30 °C, UV detection (254 nm).

The chromatogram (Figure 7) shows the separation of two homologous alkylbenzenes and nonplanar PAHs, and it was observed that all four compounds are well resolved. The retention of some PAH isomers and aromatic positional isomers was examined to assess the shape selectivity by Sil-

poly**4**, and the retention data were compared with those for the conventional ODS phase. Several size and shape parameters for PAHs were introduced for systematic investigations of retention behavior. The retention data for PAH isomers on Sil-poly**4** and their comparison with ODS are given in Table 1.

Table 1. Retention and separation factors of PAHs for Sil-poly**4** and ODS stationary phases.

Analyte[a]	Sil-poly**4**		Sil-ODS	
	k	α	k	α
benzene	0.974		0.74	
		2.36		1.78
naphthalene	2.30		1.32	
		6.30		3.55
anthracene	6.141		2.63	
pyrene	10.28		3.76	
		1.41		1.21
triphenylene	14.42		4.57	
		1.23		1.29
benzo[*a*]anthracene	12.64		4.87	
		1.43		1.30
chrysene	14.70		4.89	
		1.90		1.49
naphthacene	19.10		5.60	
cis-stilbene	3.22		2.08	
		1.44		1.05
trans-stilbene	4.63		2.20	
o-terphenyl	4.468		3.07	
		1.95		1.44
m-terphenyl	8.71		4.45	
		3.10		1.44
p-terphenyl	13.81		4.45	

[a] Mobile phase: methanol/water (90:10); column temperature: 30 °C; flow rate: 1.00 mL min^{-1}; UV detection (254 nm).

To evaluate the planarity recognition capability of ODS phases, Tanaka et al.[33] introduced the selectivity for two solutes, *o*-terphenyl ($F=9$, $L/B=1.11$) and triphenylene ($F=9$, L/B = 1.12). (Definitions of F and L/B are given in the Supporting Information.) We observed that Sil-poly**4** ($\alpha_{\text{triphenylene/}o\text{-terphenyl}}=3.23$) showed extremely enhanced molecular planarity recognition compared to ODS ($\alpha_{\text{triphenylene/}o\text{-terphenyl}}=1.4$). A typical example for selectivity towards PAHs on Sil-poly**4** is shown in Figure 8. The retention data show that Sil-poly**4** yielded higher separation for all sets of PAHs and geometrical isomers than the conventional reversed-phase HPLC stationary phase, regardless of the fact that the alkyl chain in Sil-poly**4** yielded a disordered *gauche* transformation and no inversion to ordered transformation was seen up to a temperature of 50 °C.

Conclusion

A new polymerizable *N*′-octadecyl-L-phenylalanine-derived monomer has been synthesized and found to be self-assembled by intermolecular hydrogen bonding. Structurally well-defined silica–polymer hybrid materials were prepared by initiator immobilization on a silica surface and subsequent surface-initiated ATRP by using initiator-modified particles as macroinitiators.

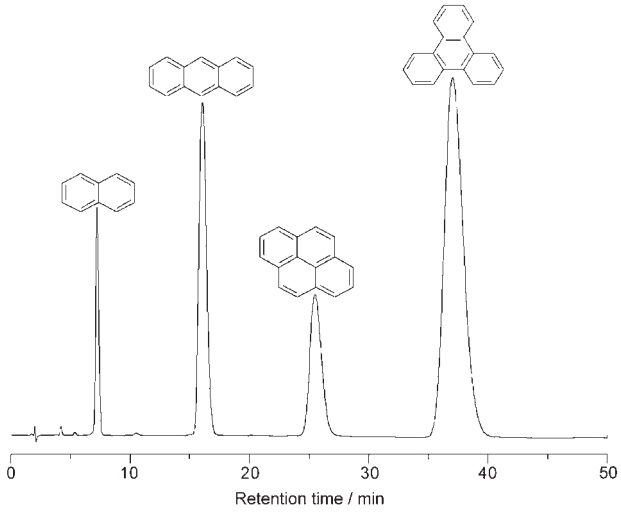

Figure 8. Chromatogram of a mixture of naphthalene, anthracene, pyrene, and triphenylene with Sil-poly**4**. Mobile phase: MeOH/H_2O (90:10), flow rate: 1 mL min^{-1}, column temperature: 30 °C, UV detection (254 nm).

The octadecyl chains on the polymer-grafted silica particles were a disordered, solid, and noncrystalline form that did not show any phase-transition behavior. Sil-poly**4** was used as a HPLC packing material and showed a reversed-phase retention mode. The chromatographic results for PAH isomers showed better separation behavior than with a conventional ODS phase. This new polymer-grafted silica could be efficiently used for the separation of PAHs in reversed-phase HPLC. Furthermore, compound **4** may also be applied towards the functionalization of magnetic particles, and the magneto-responsive composite materials ultimately could be used for magnetic hyperthermia. By introducing cationic functional groups, the **4** molecule could be a potential candidate for the preparation of carriers that can deliver nucleic acids into cells to investigate the properties of gene sequences.

Experimental Section

General methods and materials: TEA (Wako, 99+ %) was distilled over potassium hydroxide. Trichlorosilane (TCA, 97 %), 2-bromoisobutyryl bromide (Aldrich, 98 %), 10-undecene-1-ol (Aldrich, 98 %), platinum(0)-1,3-divinyl-1,1,3,3-tetramethyldisiloxane (Karstedt catalyst; Aldrich, 0.1 M in xylenes), PMDETA (Wako, 98.0 %), and copper(I) bromide (Aldrich, 99.999 %) were used as received. Toluene (Wako, 99+ %) and diethyl ether (Wako, 99.5+ %) were distilled from sodium/benzophenone and stored under argon when not used. Porous silica particles (YMC-GEL) were purchased from YMC (Kyoto, Japan); their average diameter, pore size, and surface area were 5 μm, 12 nm, and 300 m^2 g^{-1}, respectively.

HPLC-grade methanol and PAH samples were obtained from Nacalai Tesque (Japan). Analytical thin-layer chromatography was performed on 0.25 mm silica gel plates, and silica gel column chromatography was car-

ried out with silica gel 60 (Wakogel C-300). IR measurements were conducted on a Jasco (Japan) FTIR-4100 Plus instrument in KBr. For DRIFT measurements, the accessory DR PRO410-M (Jasco, Japan) was used. TGA was performed on a Seiko EXSTAR 6000 TG/DTA 6300 thermobalance in static air from 30 to 800 °C at a heating rate of 10 °C min^{-1}. For characterization of synthesis, ^{1}H and ^{13}C NMR spectra were recorded on a JEOL JNM-LA400 (Japan) instrument. Chemical shifts (δ) of ^{1}H and ^{13}C were expressed in parts per million (ppm) with use of the internal standard Me_4Si ($\delta = 0.00$ ppm). Coupling constants (J) are reported in Hertz. Elemental analyses were carried out on a Perkin–Elmer CHNS/O 2400 apparatus. UV/Vis spectra were measured on a Jasco V-560 spectrophotometer by using a quartz cell of width 1 cm.

Solid- (^{13}C CP/MAS NMR and ^{29}Si CP/MAS NMR) and suspended-state ^{1}H NMR measurements: NMR spectra were measured by a Varian UnityInova AS400 instrument at a static magnetic field of 9.4 T by using a GHX nanoprobe for suspension-state NMR and a solid probe for CP/MAS NMR spectroscopy at a spin rate of 2000–3500 Hz for suspension-state NMR and 4000–4500 Hz for solid-state NMR measurements. The samples for suspension-state ^{1}H NMR spectroscopy were made by using Sil-poly**4** (10 mg) in CD_3OD (100 μL) with tetramethylsilane (0.03 %). ^{1}H NMR spectra were recorded at 20–50 °C at 5 °C intervals by using a GHX Varian AS400 nanoprobe. The parameters used for measurement were delay time 1.5 s, pulse width 2.2 μs, transient number 32, and spectral width 6000 Hz. Water was suppressed by using a presaturation pulse sequence with a saturation delay of 1.5 s and a saturation power of 2 dB. For assigning peaks, after determination of a pulse width of 90°, simple RELAY COSY (correlation spectroscopy test) was carried out and the chemical shifts of the terminal methyl and methylene proton of the alkyl chain were determined. For solid-state ^{13}C CP/MAS, the NMR measuring parameters were: spectral width 50000 Hz, proton pulse width 90° = 11.6 μs, contact time for cross polarization 5 ms, and delay before acquisition 2 s. High-power proton decoupling of 63 dB with fine attenuation of dipole $r = 2500$ was used only during detection periods. ^{29}Si CP/MAS NMR spectra were collected with the same instrument. Representative samples (200–250 mg) were spun at 3500 Hz by using 7 mm double-bearing ZrO_2 rotors. The spectra were obtained with a cross-polarization contact time of 5 ms. The pulse interval time was 1.5 s. The transmitter frequencies of ^{29}Si and ^{1}H were 59.59 and 300.13 MHz, respectively. Typically, 1.5-k FIDs with an acquisition time of 30 ms were accumulated in 1 kilobyte (kb) data points and zero filling to 8 kb prior to Fourier transformation. The line broadening used was 30 Hz and the spectral width for all spectra was about 25 kHz.

HPLC measurement: The chromatographic system consisted of a Gulliver PU-980 intelligent HPLC pump, a Rheodyne sample injector with a 20 μL loop, and a Jasco multiwavelength UV detector MD 2010 plus. The column temperature was maintained by using a column jacket that had a circulator with a heating and a cooling system. A personal computer connected to the detector with Jasco–Borwin (Ver 1.5) software was used for system control and data analysis. As the sensitivity of the UV detector was high, 5 μL of sample solution was used for each injection. To avoid overloading effects, special attention was given to the selection of optimum experimental conditions. Separations were performed with HPLC-grade methanol/water (90:10) as mobile phase at a flow rate of 1.00 mL min^{-1}. Measurement of the retention factor (k) was carried out under isocratic elution conditions. The separation factor (α) is the ratio of the retention factor of two solutes that are being analyzed. The retention time of D_2O was used as the void volume (t_0) marker (the absorption of D_2O was measured at 400 nm, which is actually considered as injection shock). All data points were derived from at least triplicate measurements, with the value of retention time (t_R) varying by ±1 %. The water/1-octanol partition coefficient (P) was measured by retention studies with ODS (monomeric; Inertsil ODS, 250×4.6 mm i.d., GL Science, Tokyo, Japan): $\log P = 3.579 + 4.207 \log k\,(r)\,0.999997$).[34]

Synthesis of L-phenylalanine-derived self-assembling monomeric organogelator

*N-Carbobenzoyl-L-phenylalanine (**1**)*: L-Phenylalanine (45 g, 272.4 mmol) was dissolved in NaOH solution (2 M, 250 mL) and stirred in an ice bath at 0 °C. Z-Cl (10.5 mL, 61.5 mmol) was added dropwise followed by the addition of NaOH (2 M, 20 mL). The addition of Z-Cl and NaOH was repeated four more times at 15 min intervals. After completion of Z-Cl addition the mixture was stirred for 1 h at 0 °C and 5 h at room temperature. The reaction mixture was extracted with diethyl ether (3×50 mL) to remove unreacted Z-Cl and the aqueous layer was separated. HCl (6 M) was added to the aqueous layer until the pH reached 2.00. The mixture was extracted with ethyl acetate (5×50 mL); the organic layer was then washed with distilled water (5×50 mL), dried over Na_2SO_4, and concentrated under reduced pressure. *n*-Hexane (300 mL) was added and the mixture was stirred with a glass rod until white crystals appeared, then kept in a refrigerator for 24 h. The white solid obtained was isolated by filtration and dried in vacuo to give **1** (83.2 g, yield: 85.6 %). M.p. 79–80 °C; ^{1}H NMR (400 MHz, $CDCl_3$): $\delta = 7.33$ (m, 5H; C_6H_5), 7.25 (m, 5H; C_6H_5), 5.13 (d, $J = 8.76$ Hz, 1H; *CHN*H*C(O)), 5.10 (s, 2H; C(O)CH_2C$_6$H$_5$), 4.70 (m, 1H; *C*H*) 3.18 (dd, $J = 8.76$ Hz, 1H; *CHC*H*), 3.08 ppm (dd, $J = 8.76$ Hz, 1H; *CHC*H*); ^{13}C NMR (100 MHz, $CDCl_3$): $\delta = 176.26$, 155.83, 136.02, 135.41, 129.30, 128.65, 128.51, 128.22, 128.08, 127.21, 127.04, 67.14, 54.55, 37.68 ppm; IR (KBr): $\tilde{\nu} = 3329$, 3150, 3087, 3063, 3033, 1718, 1698, 1531, 1496, 1454 cm^{-1}; elemental analysis calcd (%) for $C_{17}H_{17}NO_4$: C 68.21, H 5.73, N 4.68; found C 67.93, H 5.81, N 4.58.

*N′-Octadecyl-N$^{\alpha}$-carbobenzoyl-L-phenylalanineamide (**2**)*: *N*-Carbobenzoyl-L-phenylalanine (**1**) (30.0 g, 100.23 mmol) and stearylamine (29.65 g, 110.25 mmol) were dissolved in dry THF (300 mL) by stirring. Anhydrous TEA (25.30 g, 250.58 mmol) was added to the mixture followed by DEPC (17.98 g, 110.25 mmol) and stirring was continued for 1 h at 0 °C. The ice bath was removed and the mixture was stirred overnight at room temperature. The mixture was concentrated under reduced pressure and the residue was dissolved in $CHCl_3$ (250 mL). The chloroform solution was washed with 10 % $NaHCO_3$ solution, HCl (0.2 M), and distilled water. The solution was dried over Na_2SO_4, concentrated under reduced pressure, recrystallized from methanol, and dried in vacuo to give a white powder (40.1 g, yield: 72.5 %). M.p. 122–123 °C; ^{1}H NMR (400 MHz, $CDCl_3$): $\delta = 7.33$ (m, 5H; C_6H_5), 7.25 (m, 5H; C_6H_5), 5.46 (s; N*H*C(O)*CH), 5.35 (s, 1H; *CHN*H*C(O)), 5.09 (s, 2H; C(O)CH_2C$_6$H$_5$)), 4.28 (t, $J = 13.6$ Hz; *C*H*), 2.95 (m, 2H; *CHCH_2C$_6$H$_5$), 3.10 (m, 2H; CH_2NHC(O)*CH), 1.55 (m, 2H; CH$_2$CH_2CH$_2$NHC(O)*CH), 1.25 (m, 30H; CH$_3$CH_2×15), 0.86 ppm (t, $J = 12.0$ Hz, 3H; CH_3); ^{13}C NMR (100 MHz, $CDCl_3$): $\delta = 170.41$, 155.83, 136.82, 136.14, 129.29, 128.70, 128.54, 128.21, 128.02, 127.03, 67.03, 56.53, 39.70, 39.53, 31.91, 29.68, 29.64, 29.57, 29.53, 29.48, 29.34, 29.26, 29.20, 26.91, 26.74, 22.68, 14.10 ppm; IR (KBr): $\tilde{\nu} = 3302$, 3150, 3087, 3063, 3033, 2919, 2849, 1686, 1654, 1534, 1467, 1439 cm^{-1}; elemental analysis calcd (%) for $C_{35}H_{54}N_2O_3$: C 76.30, H 9.88, N 5.09; found C 76.30, H 9.80, N 5.13.

*N′-Octadecyl-L-phenylalanineamide (**3**)*: *N′*-Octadecyl-N$^{\alpha}$-carbobenzoyl-L-phenylalanineamide (**2**) (14.0 g, 25.41 mmol) was dissolved in ethanol (300 mL) with heating and Pd carbon black (1.4 g) was added to the solution. H_2 gas was bubbled slowly into the solution for 4 h at 60 °C. The Pd carbon black was removed by filtration, then the solution was concentrated under reduced pressure, recrystallized from methanol, and dried in vacuo to give a white powder (7.8 g, yield: 73.65 %). M.p. 78–79 °C; ^{1}H NMR (400 MHz, $CDCl_3$): $\delta = 7.21$ (m, 5H; C_6H_5), 3.57 (q, $J = 16$ Hz; *C*H*), 3.21–3.29 (m, 3H; CH_2NHC(O)*CH, *CHCHC$_6$H$_5$), 2.66 (q, $J = 23.4$ Hz, 1H; *CHCHC$_6$H$_5$), 1.47 (d, $J = 6.8$ Hz, 2H; CH$_2$CH_2CH$_2$NHC(O)*CH), 1.25 (m, 30H; CH$_3$CH_2×15), 0.86 ppm (t, $J = 13.4$ Hz, 3H; CH_3); ^{13}C NMR (100 MHz, $CDCl_3$): $\delta = 173.9$, 137.98, 129.29, 128.66, 126.75, 56.46, 41.05, 39.09, 31.90, 29.67, 29.63, 29.57, 29.56, 29.53, 29.34, 29.29, 26.92, 22.66, 14.09 ppm; IR (KBr): $\tilde{\nu} = 3366$, 3295, 3087, 3063, 3030, 2956, 2918, 2849, 1635, 1550, 1471 cm^{-1}; elemental analysis calcd (%) for $C_{27}H_{48}N_2O$: C 77.82, H 11.61, N 6.73; found: C 77.53, H 11.38, N 6.75.

*N′-Octadecyl-N$^{\alpha}$-(4-vinyl)-benzoyl-L-phenylalanineamide (**4**)*: *N′*-Octadecyl-L-phenylalanineamide (**3**) (5.0 g, 12.00 mmol) and 4-vinylbenzoic acid (2.0 g, 13.2 mmol) were dissolved in dry THF (200 mL) and stirred. Anhydrous TEA (3.03 g, 30.2 mmol) was added followed by DEPC (2.2 g, 13.2 mmol) and stirring was continued for 1 h at 0 °C in an ice bath. The mixture was stirred at room temperature overnight, then concentrated under reduced pressure and the residue was dissolved in $CHCl_3$

(150 mL). The chloroform solution was washed with 10% $NaHCO_3$, HCl (0.2 M) and distilled water (3×50 mL) and then the organic layer was dried over Na_2SO_4. The mixture was concentrated and recrystallized from ethanol and dried in vacuo to give a white powder (6.0 g, yield: 91.5%). M.p. 137–138 °C; ^{1}H NMR (400 MHz, $CDCl_3$): δ = 7.70 (d, J = 8.76 Hz, 2H; C_6H_5), 7.4 (d, J = 8.76 Hz, 2H; C_6H_5), 7.3 (m, 5H; C_6H_5), 7.23 (d, J = 5.88 Hz, 1H; *CHN*HC*(O)), 6.70 (q, J = 28.32 Hz, 1H; $C_6H_5CHCH_2$), 5.8 (d, J = 17.56 Hz, 1H; C_6H_5CHCH-H), 5.5 (s, 1H; CH_2-N*H*-C(O)*CH), 5.34 (d, J = 10.8 Hz, 1H; C_6H_5CHCH-*H*), 4.73 (t, J = 9.6 Hz; *C*H*), 3.25 (m, 1H; CH_2NHC(O)*CH), 3.03 (m, 2H; *CHC$H_2C_6H_5$), 1.30 (m, 32H; $CH_3CH_2\times16$), 0.86 ppm (t, J = 12.0 Hz, 3H; CH_3); ^{13}C NMR (100 MHz, $CDCl_3$): δ = 170.60, 166.70, 140.97, 136.92, 135.93, 132.90, 129.39, 128.71, 127.40, 127.05, 126.33, 116.08, 55.21, 39.62, 38.91, 31.94, 29.72, 29.67, 29.61, 29.52, 29.37, 29.30, 29.25, 26.81, 22.70, 14.11 ppm; IR (KBr): $\tilde{\nu}$ = 3306, 3087, 3063, 3033, 2919, 2850, 1658, 1631, 1532, 1503, 1470 cm^{-1}; elemental analysis calcd (%) for $C_{36}H_{54}N_2O_2$: C 79.06, H 9.96, N 5.12; found C 78.65, H 9.83, N 5.02.

Immobilization of initiator 5 on silica particles: Silica (5 g) was suspended in toluene (30 mL) in a round-bottomed flask, [11-(2-bromo-2-methyl)propionyloxy]undecyltrichlorosilane (**5**; 2.150 g, 4.72 mmol) was added and the suspension was rotated for 5 min. Then Et_3N (1.44 g, 14.2 mmol) was added and the rotation was continued under an inert atmosphere for 24 h. Silica particles were separated, washed with toluene, methanol, water, methanol, and diethyl ether (each three times), and stored at room temperature before polymerization.

Surface-initiated ATRP from Sil-5: Initiator-grafted silica (Sil-**5**; 4.1 g), compound **4** (3.94 g, 7.2 mmol,) and PMDETA (0.536 g, 3.1 mmol) were suspended in dry toluene (17 mL) and the suspension was purged with nitrogen. CuBr (0.085 g, 2.02 mmol) was added and the mixture was degassed by three freeze–pump–thaw cycles. The flask was then placed in an oil bath with a preset temperature of 90 °C and rotation at a slow velocity was maintained for 24 h. The reaction mixture was cooled to room temperature, filtered, and the residue was washed with hot toluene, hot chloroform, and methanol repeatedly. For separation of the remaining catalyst,[35] the particles were placed in a round-bottomed flask, suspended in a mixture of methanol and an aqueous solution of K_2EDTA (0.25 M), and the flask was rotated at 40 °C for 6 h. After filtration, the silica particles were washed with water, methanol, and diethyl ether and dried under vacuum.

Acknowledgements

M.M.R. and M.C. acknowledge the Japan Society for the Promotion of Science (JSPS) for providing postdoctoral fellowships (ID P06076, P06357) and giving financial support to carry out this research project.

[1] a) H. A. Klok, J. F. Langenwalter, S. Lecommandoux, *Macromolecules* **2000**, *33*, 7819–7826; b) H. Schlaad, H. Kukula, B. Smarsly, M. Antonietti, T. Pakula, *Polymer* **2002**, *43*, 5321–5328; c) G. Floudas, P. Papadopoulos, H. A. Klok, G. W. M. Vandermeulen, J. Rodriguez-Hernandez, *Macromolecules* **2003**, *36*, 3673–3683.

[2] a) B. S. Li, K. K. L. Cheuk, L. Ling, J. Chen, X. Xiao, C. Bai, B. Z. Tang, *Macromolecules* **2003**, *36*, 77–85; b) I. W. Hamley, A. Ansari, V. Castelletto, H. Nuhn, A. Rosler, H. A. Klok, *Biomacromolecules* **2005**, *6*, 1310–1315; c) J. J. L. M. Cornelissen, A. E. Rowan, R. J. M. Nolte, N. A. J. M. Sommerdijk, *Chem. Rev.* **2001**, *101*, 4039–4070.

[3] T. Oishi, Y. K. Lee, A. Nakagawa, K. Onimura, H. Tsutsumi, *J. Polym. Sci. Part A: Polym. Chem.* **2002**, *40*, 1726–1741.

[4] A. Lekchiri, J. Morcellet, M. Morcellet, *Macromolecules* **1987**, *20*, 49–53.

[5] R. Barbucci, M. Casolaro, A. Magnani, *J. Controlled Release* **1991**, *17*, 79–88.

[6] A. Bentolila, I. Vlodavsky, R. Ishai-Michaeli, O. Kovalchuk, C. Haloun, A. J. Domb, *J. Med. Chem.* **2000**, *43*, 2591–2600.

[7] a) T. J. Deming, *Nature* **1997**, *390*, 386–389; b) T. J. Deming, *J. Polym. Sci. Part A: Polym. Chem.* **2000**, *38*, 3011–3018; c) A. Nagai, D. Sato, J. Ishikawa, B. Ochiai, H. Kudo, T. Endo, *Macromolecules* **2004**, *37*, 2332–2334; d) Y. Mei, K. L. Beers, M. H. C. Byrd, D. L. VanderHart, N. R. Washburn, *J. Am. Chem. Soc.* **2004**, *126*, 3472–3476; e) T. E. Hopkins, K. B. Wagener, *Macromolecules* **2004**, *37*, 1180–1189; f) G. Gao, F. Sanda, T. Masuda, *Macromolecules* **2003**, *36*, 3932–3937; g) F. Sanda, H. Araki, T. Masuda, *Macromolecules* **2004**, *37*, 8510–8516.

[8] F. Sanda, T. Endo, *Macromol. Chem. Phys.* **1999**, *200*, 2651–2661.

[9] a) K. P. Krenkler, R. Laible, K. Hamann, *Angew. Makromol. Chem.* **1953**, *53*, 101; b) N. Tsubokawa, M. Hosoya, K. Yanadori, Y. Sone, *J. Macromol. Sci. Part A: Pure Appl. Chem.* **1990**, *A27*, 445; c) N. Tsubokawa, A. Kuroda, Y. Sone, *J. Polym. Sci.* **1989**, *27*, 1701–1712; d) H. Ben Ouada, H. Hommel, A. P. Legrand, H. Balard, E. Papirer, *J. Colloid Interface Sci.* **1988**, *122*, 441–449; e) K. Bridger, B. Vincent, *Eur. Polym. J.* **1980**, *16*, 1017–1021; f) M. Takafuji, S. Ide, H. Ihara, Z. Xu, *Chem. Mater.* **2004**, *16*, 1977–1983.

[10] M. Husseman, E. E. Malmström, M. McNamara, M. Mate, D. Mecerreyes, D. G. Benoit, J. L. Hedrick, P. Mansky, E. Huang, T. P. Russell, C. J. Hawker, *Macromolecules*, **1999**, *32*, 1424–1431.

[11] a) A. Ulman, *Chem. Rev.* **1996**, *96*, 1533–1554; b) O. Prucker, J. Rühe, *Macromolecules* **1998**, *31*, 602–613; c) O. Prucker, J. Rühe, *Langmuir* **1998**, *14*, 6893–6898; d) J. Habicht, M. Schmidt, J. Rühe, D. Johannsmann, *Langmuir* **1999**, *15*, 2460–2465; e) M. Ruths, D. Johannsmann, J. Rühe, W. Knoll, *Macromolecules* **2000**, *33*, 3860–3870; f) D. Cossement, Y. Delrue, Z. Mekhalif, J. Delhalle, L. Hevesi, *Surf. Interface Anal.* **2000**, *30*, 56–60; g) D. Cossement, C. Pierard, J. Delhalle, J.-J. Pireaux, L. Hevesi, Z. Mekhalif, *Surf. Interface Anal.* **2001**, *31*, 18–22; h) D. Cossement, F. Plumier, J. Delhalle, L. Hevesi, Z. Mekhalif, *Synth. Met.* **2003**, *138*, 529–536; i) D. Cossement, Z. Mekhalif, J. Delhalle, L. Hevesi in *Organosilicon Chemistry VI, Vol. 2* (Eds.: N. Auner, J. Weis), Wiley-VCH, Weinheim, **2005**, pp. 999–1005.

[12] W. A. Braunecker, K. Matyjaszewski, *Prog. Polym. Sci.* **2007**, *32*, 93–146.

[13] *Controlled Living Radical Polymerization: Progress in ATRP, NMP and RAFT, Vol. 768* (Ed.: K. Matyjaszewski), American Chemical Society, Washington, DC, **2000**.

[14] a) J. S. Wang, K. Matyjaszewski, *J. Am. Chem. Soc.* **1995**, *117*, 5614–5615; b) M. Kato, M. Kamigato, M. Sawamoto, T. Higashimura, *Macromolecules* **1995**, *28*, 1721–1723.

[15] K. Matyjaszewski, T. P. Davis, *Handbook of Radical Polymerization*, Wiley-Interscience, New York, **2002**.

[16] a) C. Allen, D. Maysinger, A. Eisenberg, *Colloids Surf. B* **1999**, *16*, 3–27; b) P. L. Soo, L. B. Luo, D. Maysinger, A. Eisenberg, *Langmuir* **2002**, *18*, 9996–10004; c) N. Nishiyama, Y. Bae, K. Miyata, S. Fukushima, K. Kataoka, *Drug Discovery Today* **2005**, *2*, 21–26; d) R. Duncan, *Nat. Rev. Drug Discovery* **2003**, *2*, 347–360; e) G. S. Kwon, T. Okano, *Adv. Drug Deliv. Rev.* **1996**, *21*, 107–116.

[17] a) P. Terech, R. G. Weiss, *Chem. Rev.* **1997**, *97*, 3133–3159; b) J. H. van Esch, B. L. Feringa, *Angew. Chem.* **2000**, *112*, 2351–2354; *Angew. Chem. Int. Ed.* **2000**, *39*, 2263–2266; c) K. Hanabusa, H. Nakayama, M. Kimura, H. Shirai, *Chem. Lett.* **2000**, *29*, 1070–1071; d) R. P. Lyon, W. M. Atkins, *J. Am. Chem. Soc.* **2001**, *123*, 4408–4413; e) S. Kiyonaka, S. Shinkai, I. Hamachi, *Chem. Eur. J.* **2003**, *9*, 976–983; f) W. Gu, L. Lu, G. B. Chapman, R. G. Weiss, *Chem. Commun.* **1997**, 543–544; g) S. Kobayashi, K. Hanabusa, N. Hamasaki, M. Kimura, H. Shirai, S. Shinkai, *Chem. Mater.* **2000**, *12*, 1523–1525; h) S. Kobayashi, N. Hamasaki, M. Suzuki, M. Kimura, H. Shirai, K. Hanabusa, *J. Am. Chem. Soc.* **2002**, *124*, 6550–6551.

[18] a) W. Klemperer, M. W. Cronyn, A. H. Maki, G. C. Pimentel, *J. Am. Chem. Soc.* **1954**, *76*, 5846–5848; b) S. H. Gellman, G. P. Dado, G. B. Liang, B. R. Adams, *J. Am. Chem. Soc.* **1991**, *113*, 1164–1173; c) G. P. Dado, S. H. Gellman, *J. Am. Chem. Soc.* **1993**, *115*, 4228–4245.

[19] K. Tomioka, T. Sumiyoshi, S. Narui, Y. Nagaoka, A. Iida, Y. Miwa, T. Taga, M. Nakano, T. Handa, *J. Am. Chem. Soc.* **2001**, *123*, 11817–11818.

[20] a) N. Yamada, T. Imai, E. Koyama, *Langmuir* **2001**, *17*, 961–963; b) X. Wang, Y. Shen, Y. Pan, Y. Liang, *Langmuir* **2001**, *17*, 3162–3167.
[21] a) M. Pursch, S. Strohschein, H. Handel, K. Albert, *Anal. Chem.* **1996**, *68*, 386–393; b) A. E. Tonelli, F. C. Schiling, F. A. Bovey, *J. Am. Chem. Soc.* **1984**, *106*, 1157–1158; c) M. Pursch, L. C. Sander, K. Albert, *Anal. Chem.* **1996**, *68*, 4107–4113.
[22] a) H. Ihara, T. Sagawa, Y. Goto, S. Nagaoka, *Polymer* **1999**, *40*, 2555–2560; b) H. Ihara, H. Tanaka, M. Shibata, S. Sakaki, C. Hirayama, *Chem. Lett.* **1997**, *26*, 113–114; c) H. Ihara, Y. Goto, T. Sakurai, M. Takafuji, T. Sagawa, S. Nagaoka, *Chem. Lett.* **2001**, *30*, 1252–1253.
[23] a) H. Ihara, M. Takafuji, C. Hirayama, D. F. O'Brien, *Langmuir* **1992**, *8*, 1548–1553; b) H. Ihara, H. Hachisako, C. Hirayama, K. Yamada, *J. Chem. Soc. Chem. Commun.* **1992**, *17*, 1244–1245; c) H. Ihara, M. Yoshitake, M. Takafuji, T. Yamada, T. Sagawa, C. Hirayama, H. Hachisako, *Liq. Cryst.* **1999**, *26*, 1021–1027.
[24] a) M. Takafuji, M. M. Rahman, M. Derakshan, H. R. Ansarian, H. Ihara, *J. Chromatogr. A* **2005**, *1074*, 223–228; b) M. M. Rahman, M. Takafuji, H. R. Ansarian, H. Ihara, *Anal. Chem.* **2005**, *77*, 6671–6681; c) M. M. Rahman, M. Takafuji, H. Ihara, *J. Chromatogr. A* **2006**, *1119*, 105–114.
[25] K. Matyjaszewski, P. J. Miller, N. Shukla, B. Immaraporn, A. Gelman, B. B. Luokala, T. M. Siclovan, G. Kickelbick, T. Vallant, H. Hoffmann, T. Pakula, *Macromolecules* **1999**, *32*, 8716–8724.
[26] M. Chamberg, R. Parnas, Y. Cohen, *J. Appl. Polym. Sci.* **1989**, *37*, 2921–2931.
[27] *The Chemistry of Silica: Solubility, Polymerization, Colloid and Surface Properties and Biochemistry* (Ed.: R. K. Iler), Wiley, New York, **1979**.
[28] a) G. Laurelle, J. Parvole, J. Francois, L. Billon, *Polymer* **2004**, *45*, 5013–5020; b) J. H. Maas, M. A. Cohen Stuart, A. B. Sieval, H. Zuilhof, E. J. R. Sudhölter, *Thin Solid Films* **2003**, *426*, 135–139.
[29] H. R. Ansarian, M. Derakhshan, M. M. Rahman, T. Sakurai, M. Takafuji, H. Ihara, *Anal. Chim. Acta* **2005**, *547*, 179–187.
[30] T. I. Korányi, J. B. Nagy, *J. Phys. Chem. B* **2005**, *109*, 15791–15797.
[31] a) A. Shundo, T. Sakurai, M. Takafuji, S. Nagaoka, H. Ihara, *J. Chromatogr. A* **2005**, *1073*, 169–174; b) H. Ihara, W. Dong, T. Mimaki, M. Nishihara, T. Sakurai, M. Takafuji, S. Nagaoka, *J. Liq. Chromatogr.* **2003**, *26*, 2473–2485; c) H. A. Claessens, M. A. Van Straten, C. A. Cramers, M. Jezierska, B. Buszewski, *J. Chromatogr. A* **1998**, *826*, 135–156; d) P. C. Sadek, P. W. Carr, *J. Chromatogr. Sci.* **1983**, *21*, 314–320.
[32] K. Kimata, K. Iwaguchi, S. Onishi, K. Jinno, R. Eksteen, K. Hosoya, M. Araki, N. Tanaka, *J. Chromatogr. Sci.* **1989**, *27*, 721–728.
[33] a) N. Tanaka, Y. Tokuda, K. Iwaguchi, J. Araki, *J. Chromatogr.* **1982**, *239*, 761–771; b) K. Kimata, K. Iwaguchi, S. Onshi, K. Jinno, R. Eksteen, K. Hosoya, M. Araki, N. Tanaka, *J. Chromatogr. Sci.* **1989**, *27*, 721–728.
[34] Y. Goto, K. Nakashima, K. Mitsushi, M. Takafuji, S. Sakaki, H. Ihara, *Chromatographia* **2002**, *56*, 19–23.
[35] Y. Shen, H. Tang, S. Ding, *Prog. Polym. Sci.* **2004**, *29*, 1053–1078.

Received: August 22, 2007
Published online: ■■ ■■, 2007

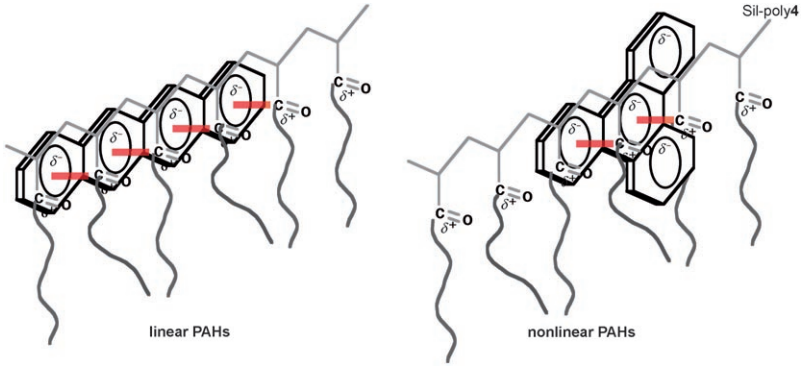

Pack it in: An L-phenylalanine-based vinylic monomer (**4**) self-assembles by hydrogen bonding. Its surface-initiated radical polymerization can be carried out from silica particles to produce a stationary phase (Sil-poly**4**) for HPLC applications. The chromatographic performance of Sil-poly**4** for polyaromatic hydrocarbons (PAHs; see figure) shows higher selectivity than conventional reversed-phase HPLC packing materials.

Liquid Chromatography

*M. M. Rahman, M. Czaun, M. Takafuji, H. Ihara** ..... ▮▮▮▮–▮▮▮▮

Synthesis, Self-Assembling Properties, and Atom Transfer Radical Polymerization of Alkylated L-Phenylalanine-Derived Monomeric Organogel from Silica: A New Approach To Prepare Packing Materials for High-Performance Liquid Chromatography